Nigerian Research Journal of Chemical Sciences (ISSN: 2682-6054)
Volume 12, Issue 2, 2024

Synthesis, Characterization and *In Vitro* Chemotherapeutic Evaluation of N,N-Donor Dihydrazone Complexes

*Sadi A. Hassan, Habu N. Aliyu and Mustapha D. Garba
Department of Pure and Industrial Chemistry, Bayero University, Kano, Nigeria
*Corresponding Author: sahassan.chm@buk.edu.ng

Accepted: November 6, 2024. Published Online: November 20, 2024

ABSTRACT

Microbial infections are life-threatening diseases. They deteriorate most disease conditions. The burden of infections due to antimicrobial resistance, especially in Africa and Asia, is alarming. Complexes of dihydrazone derived from oxalyldihydrazide and piperonaldehyde were synthesized by conventional salvo-thermal method and characterized by spectral and physicochemical techniques. The effective magnetic moment values indicate the paramagnetic behaviour of Ni(II) and Cu(II) complexes in an octahedral environment, whereas, Zn(II) complex is diamagnetic. UV-visible spectra show π - π^* and n - π^* transitions between 206 – 285 nm and 336 – 383 nm respectively. The infrared spectrum of the dihydrazone showed C=N absorption band at 1603 cm^{-1} which was shifted to 1626 – 1629 cm^{-1} in the spectra of the complexes due to coordination through N-atoms of azomethine groups. The mass spectrum of the dihydrazone B displayed the molecular ion peak at m/z 383 in a positive mode due to $[M + H]^+$ ion, The TGA curve of dihydrazone B revealed two sequential stages of weight loss at different temperatures indicated by a DTGA curve. Elemental analyses results were in good agreement with the calculated percentage values of C, H and N in the compounds, confirming the proposed structures. The complexes show significant antimicrobial activities and considerable antioxidant and anti-inflammatory potency than the free dihydrazone.

Keywords: Anti-inflammatory, Antioxidant, Dihydrazone, TGA/DTGA and UV-visible

INTRODUCTION

The number of people suffering from life-threatening multidrug-resistant infections is increasing in both developed and developing nations, leaving humanity without any choice but to search for new treatment options and strategies [1]. Drug resistance is a well-known phenomenon that results when diseases refuse to respond to pharmaceutical treatments. Although several classes of antibacterial and antifungal compounds are presently available, the resistance of microorganisms to these drugs has been constantly emerging [2]. To address

the severe challenges of multidrug resistance in treating bacterial and fungal infections there is need to discover new drugs with novel mechanisms of action, higher activity and improved selectivity. Microbial infections are life-threatening diseases, they weaken the immune system and deteriorate most disease conditions. The burden of infections due to antimicrobial resistance, especially in Africa and Asia, is alarming. The use of conventional antibiotics as both preventive and curative measures against microbes has increased multidrug-resistant infections that have negatively impacted human being of all age categories [3]. According to the European Center for Disease Prevention and Control, about 33,000 people die annually from infections [4-5]. Antibiotic-resistant bacteria are among the underlying conditions that have been increasing the mortality rate to date. Millions of people have been affected. According to the World Health Organization, most approved antibiotics are inefficient in treating bacterial infections due to their ability to form biofilms, regularly change strains, and develop complex structures with other pathogens [3].

Hydrazones and their complexes are bioactive compounds and have encouraged synthetic researchers in the field of pharmacological chemistry to explore their potential applications [6]. It is suggested that the presence of the metal ions improves the efficiency of the complexes as potential antibacterial and antioxidant agents when compared to the free organic compound alone [4-7]. A number of metal complexes have a wide range of pharmaceutical and biological applications. For instance, complexes having “O” and “N” donor atoms are very essential due to their numerous biological applications., Antibacterial [9-10], enzyme inhibitors [11], antifungal [12-14], antitumor [15-16], antioxidants [17], anti-hypertensive [18], anticonvulsant [19], anti-inflammatory [20], anti-proliferative [21] and antimalarial agents [20-22].

This research was aimed to synthesize cost-effective, more effective, safer/benign (gastro-intestinal friendly), multi-target, biologically active complex compounds with desired chemotherapeutic properties and new mode of action, that will overcome the problem of life-threatening multidrug-resistant infections.

MATERIALS AND METHODS

Materials

All the chemicals were of analytical grade and were used without further purification. The transition metal salts and other chemicals were obtained from either Merck or Sigma Aldrich. All glass ware washed with detergent, rinsed with distilled water and dried in the oven at 110

^{o}C. All weighing was carried out using an electric balance (model AB54). Melting point and decomposition temperatures were recorded using SMP10 digital melting point apparatus.

Synthesis of Oxalyldihydrazone B

Bis(piperonaldehyde)oxalyldihydrazone was synthesized by general condensation procedure using 1:2 ratios of oxalyldihydrazide (0.00l mol, 0.1181 g) and piperonaldehyde (0.002 mol, 0.300 g) respectively. The cream compound was obtained according to the method reported by Hassan *et al.* [23].

Synthesis of Dihydrazone B Complexes

This was conducted by adopting the method reported by Ayman *et al.,* [24]. The complexes were synthesized by the conventional salvo-thermal method. The dihydrazone B (0.002 mol, 0.7642 g) was added to 60 cm^3 ethanol. The Ni(II), Cu(II) and Zn(II) chloride were separately dissolved in 30 cm^3 ethanol (0.001 mol). The solutions were transferred to a round bottom flask and refluxed for six (6) hours. After quenching the reaction, the volume was reduced to 30 cm^3 by evaporation on a water bath. The resulting reaction mixture was cooled to room temperature. The coloured solid complexes were filtered off, washed several times with cold ethanol and then dried in a desiccator over $CaCl_2$. The dried compounds were weighed to get the experimental yield.

Molar Conductivity Measurement of the Dihydrazone B Complexes in DMF

Conductivity measurement was done using Jenway conductivity meter (model 4010).

Magnetic Susceptibility Measurement

Magnetic susceptibility measurements were conducted and recorded using Sherwood magnetic susceptibility balance.

Infrared Spectral Analysis of the Dihydrazone B and its Metal(II) Complexes

Infrared spectral analysis was recorded using Fourier Transform Infrared Spectrophotometer (FTIR) (CARY 630 Agilent technology).

UV-Visible Spectral Analysis of the Dihydrazone B and its Metal(II) Complexes

The electronic spectra (UV-visible spectra) of the ligand and its complexes have been recorded between 200-600 nm at room temperature using Perkin-Elmer Lambda 35.

Micro-analytical Analysis of the Dihydrazone B and its Metal(II) Complexes

CHN Micro-analysis was conducted using Exeter CE-440 Elemental analyser.

Mass spectral Analysis

Mass spectral analysis was conducted using Ion trap mass spectrometer.

Thermogravimetric Analysis

The compounds were subjected to TGA/DTGA analysis at 15 °C/minute heating rate in an inert argon environment using TGA 5500 (Temperature range from ambient to 1000 °C).

Antimicrobial Assay

The antibacterial and antifungal activity tests of the synthesized dihydrazone and its respective complexes were carried out against three pathogenic bacterial isolates, *Staphylococcus aureus, Escherichia coli and Salmonella typhi* and three deleterious fungal isolates, *Aspergillus flavus, Aspergillus fumigitus* and *Aspergillus niger* using well diffusion method by adopting the methods reported by Mouayed and Abduljleel, [25], and Laxman *et al,* [26] with slight modification. The results are shown in Figures 1 and 2 respectively.

DPPH Radical Scavenging Assay

The stock solution of each standard control (Ascorbic acid), dihydrazone and the complexes were prepared (2 mg/mL each) and diluted to final concentration of 1000, 500, 250, 125, 62.5, 31.25, 15.63 and 7.81 µg/mL by serial dilution. A 100 µL of 0.1mM 2,2-Diphenyl-1-picrylhydrazyl radical (DPPH) was used to evaluate the antioxidant potentials of the compounds. The absorbance was recorded at 517 nm using a JASCO model V-550 UV-Vis spectrophotometer in triplicate [27]. The percentage radical scavenging activities (% RSA) were calculated by using the relation shown in equation 1.

$$\% \text{ RSA} = \frac{\text{Absorbance of Control} - \text{Absorbace of Sample}}{\text{Absorbance of Control}} \times 100 \qquad (1)$$

***In-vitro* Anti-inflammatory Evaluation**

The dihydrazone and its complexes were subjected to *in-vitro* anti-inflammatory test by protein denaturation technique at different concentrations., 62.5, 125, 250, 500, 1000 and 2000 µg/mL. The standard drug (diclofenac sodium) and the synthesized compounds were dissolved in a minimum amount of dimethylformamide (DMF) and diluted with phosphate buffer (0.2 M, pH 7.4). Final concentration of DMF in all the solution was less than 2%. About 1 mL of the test solution containing different concentrations of the compounds were mixed with 1 mL of 1 mM egg albumin solution in phosphate buffer and incubated at 37° ± 2° C for 15 min. Denaturation was induced by keeping the reaction mixture at 70° ± 2° C in water bath for 10 min. After cooling, the turbidity was measured at 660 nm. Each experiment

was done in triplicate and average is taken. Diclofenac sodium was used as standard drug (positive control) to compare its inhibition with the inhibition of test samples. The absorbance of 1 mM egg albumin solution in phosphate buffer without the test samples was taken as the absorbance of control which was used in the computation of % inhibition (Karthik *et al.,* 2024) [1]. The percentage of inhibition of denaturation was calculated using equation 2.

$$\% \text{ Inhibition } = \frac{Ac - At}{Ac} \times 100 \qquad (2)$$

Where, A_c = Absorbance of control, A_t = Absorbance of test sample

Statistical Analysis

The IC50 values of the standard drugs (ascorbic acid and diclofenac sodium), the dihydrazone and its complexes at different concentrations were statistically analysed by probit analysis using IBM SPSS software version 20 [28].

RESULTS AND DISCUSSION

The results obtained from the physico-chemical analyses, spectral characterizations and *in-vitro* pharmacological evaluation of the dihydrazone and its complexes were presented in Table 1 - 6.

Table 1: Percentage yield and some Properties of the Synthesized Compounds

Compounds	Colour	Melting Point (°C)	Decomposition Temperature (°C)	Percentage Yield (%)
Ligand B	Light yellow	217	-	84
$[NiB_2Cl_2].3H_2O$	Light brown	-	268	60
$[CuB_2Cl_2].2H_2O$	Lemon-green	-	317	53
$[ZnB_2Cl_2].4H_2O$	Cream	-	325	51

Where B = $C_{18}H_{14}N_4O_6$

Table 2: Molar Conductivity Measurement of the Dihydrazone B Complexes in DMF

Compounds	Specific Conductance ($\Omega^{-1}cm^{-1}$)	Molar Conductance ($\Omega^{-1}cm^2mol^{-1}$)
$[NiB_2Cl_2].3H_2O$	23.2×10^{-6}	23.2
$[CuB_2Cl_2].2H_2O$	31.5×10^{-6}	31.5
$[ZnB_2Cl_2].4H_2O$	12.7×10^{-6}	12.7

Where B = $C_{18}H_{14}N_4O_6$

Table 3: Magnetic Susceptibility Data of Dihydrazone Complexes.

Compounds	Xg (g^{-1})	Xm (mol^{-1})	μ_{eff} (B.M)	Magnetic property
$[NiB_2Cl_2].3H_2O$	3.7468×10^{-6}	3.5531×10^{-3}	2.91	Paramagnetic
$[CuB_2Cl_2].2H_2O$	1.3899×10^{-6}	1.2997×10^{-3}	1.76	Paramagnetic
$[ZnB_2Cl_2].4H_2O$	-4.7311×10^{-7}	-4.6034×10^{-4}	-ve	Diamagnetic

Where B = $C_{18}H_{14}N_4O_6$

Table 4: Infrared Spectral Data of the Dihydrazone B and its Metal(II) Complexes

Compounds	υ(O-H) cm^{-1}	υ(N-H) cm^{-1}	υ(C=O) cm^{-1}	υ(C=N) cm^{-1}	υ(M-N) cm^{-1}	υ(M-Cl) cm^{1}
Ligand B	-	3309	1734	1603	-	-
$[NiB_2Cl_2].3H_2O$	3327	3253	1666	1629	515	474
$[CuB_2Cl_2].2H_2O$	3365	3238	1659	1626	535	437
$[ZnB_2Cl_2].4H_2O$	3342	3253	1663	1629	540	415

Where B = $C_{18}H_{14}N_4O_6$

Table 5: UV-Visible Spectral Data of the Dihydrazone B and its Metal(II) Complexes

Compounds	π - π* (nm) Aromatic	π - π* (nm) C=O	π - π* (nm) C=N	n - π* (nm) C=O	n - π* (nm) C=N
Ligand B	206	249	268	336	383
$[NiB_2Cl_2].3H_2O$	214	253	279	369	376
$[CuB_2Cl_2].2H_2O$	207	260	284	343	367
$[ZnB_2Cl_2].4H_2O$	220	256	285	348	379

Where B = $C_{18}H_{14}N_4O_6$

Table 6: Micro-analytical Data of the Dihydrazone B and its Metal(II) Complexes

Compounds	Percentage of Elements Calculated (Found)		
	C	H	N
Ligand B	56.55 (55.28)	3.69 (3.31)	14.65 (13.66)
$[NiB_2Cl_2].3H_2O$	45.60 (43.42)	3.61 (2.98)	11.82 (9.77)
$[CuB_2Cl_2].2H_2O$	46.24 (45.11)	3.45 (3.22)	11.98 (11.39)
$[ZnB_2Cl_2].4H_2O$	44.44 (43.39)	3.73 (3.41)	11.52 (10.78)

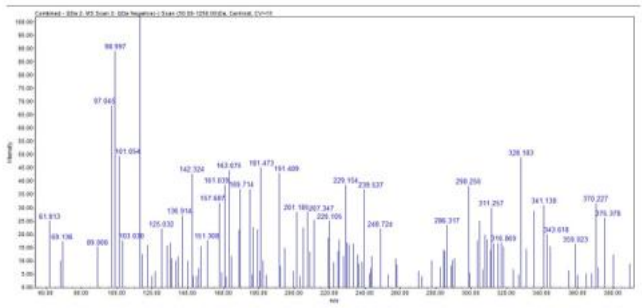

Fig.1: Mass spectrum of dihydrazone B

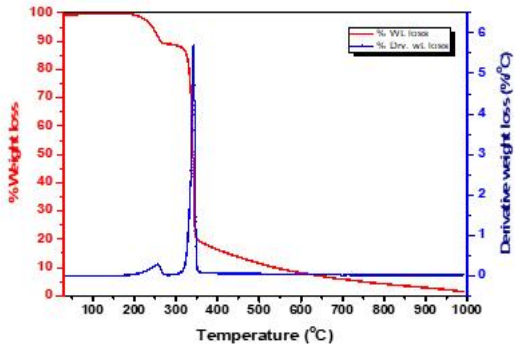

Fig. 2: Thermogram of dihydrazone B

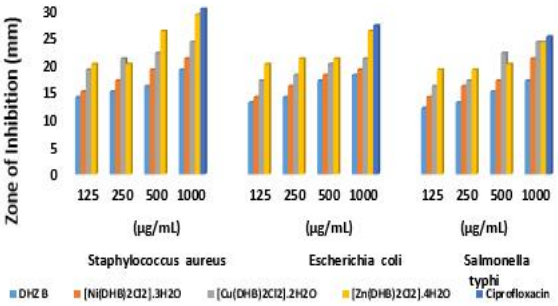

Fig. 3: Bar chart showing the antibacterial activity of dihydrazone B and its complexes

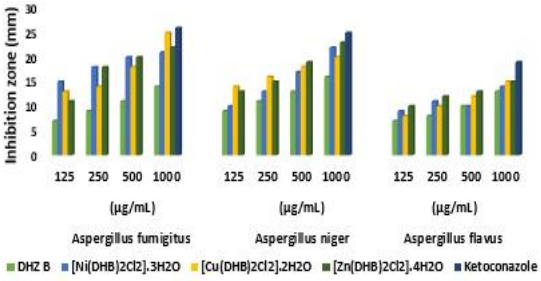

Fig. 4: Bar chart showing the antifungal activity of dihydrazone B and its complexes

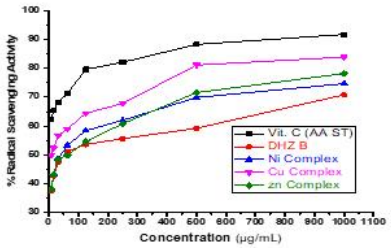

Fig. 5: Percentage RSA of ascorbic acid, dihydrazone B and its complexes

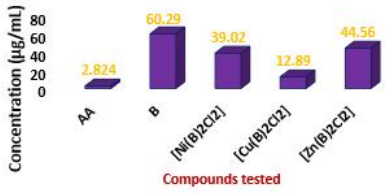

Fig. 6: Antioxidant IC50 Bar chat of ascorbic acid, dihydrazone B and its complexes
Key: AA = Ascorbic Acid

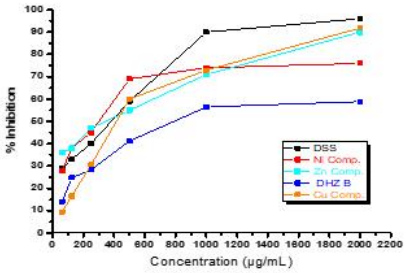

Fig. 7: Anti-inflammatory percentage inhibition of dihydrazone B and its complexes

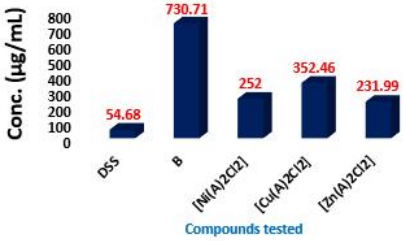

Fig. 8: Anti-inflammatory IC50 Bar-chat of diclofenac sodium, dihydrazone B and its individual complexes
Key: DSS = Diclofenac Sodium Standard

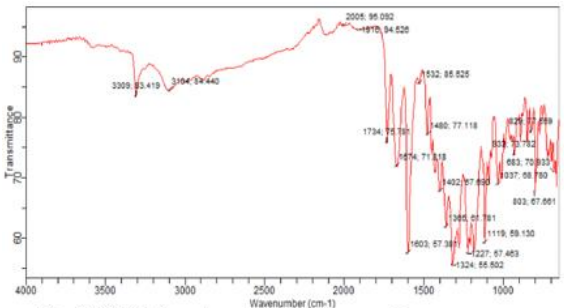

Fig. 9: FTIR Spectrum of dihydrazone B

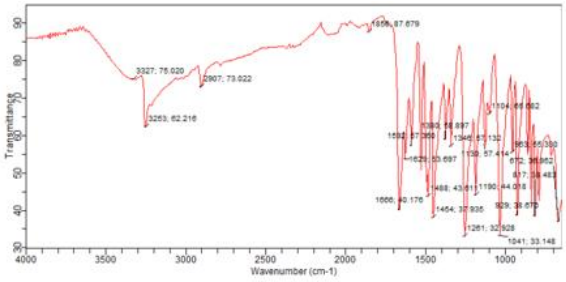

Fig. 10 FTIR Spectrum of $[NiB_2Cl_2].3H_2O$ Complex

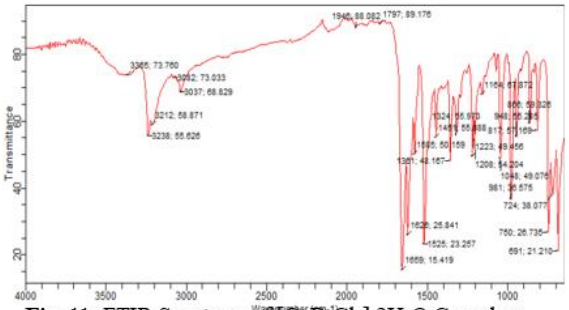

Fig. 11: FTIR Spectrum of $[CuB_2Cl_2].2H_2O$ Complex

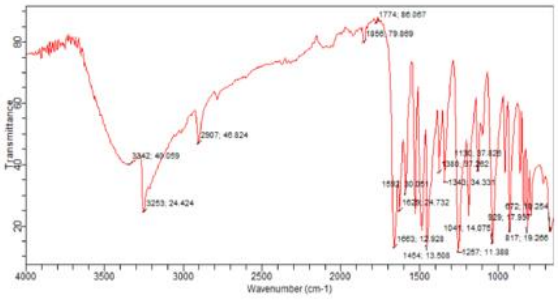

Fig. 12: FTIR Spectrum of $[ZnB_2Cl_2].4H_2O$ Complex

Table 1, show some physical properties of dihydrazone B and its respective complexes. The colour of the dihydrazone is light-yellow due to transition of electron between chromophores and lone pairs of hetero atoms. Likewise, the complexes have different colours due to varying wavelength at which they absorb light in the visible region, this is because the number of electrons in the central metal ions varies. All the complexes have relatively high decomposition temperature in the range of 268 to 325 ^oC. This indicates their good thermal stability. The stability of the complexes might be due to the chelation. The free dihydrazone has a melting point of 217 ^oC, which are in good agreement with the results reported by Suleiman *et al.,* [29]. The dihydrazone yield was excellent 84 %. The high yield indicate that the reaction is economically feasible and promising, so also the condition for the reaction is technically feasible. All the synthesized complexes were found to have good percentage yield in the range of 51 to 60 % and comparable to the results reported by Khaleel *et al.,* [30]. The molar conductance measurement of metal (II) complexes, were carried out in DMF and the values obtained were in the range of 12.7 - 31.5 $\Omega^{-1}cm^2mol^{-1}$. The values were presented in Table 2. The low values of molar conductance suggested the non-electrolytic behaviour of all the complexes. Since the dihydrazone is a neutral ligand and all the metal ions were in +2 state, this further confirmed that the two chloride ions were inside the coordination sphere [33].

Table 3 displays the magnetic susceptibility measurement results of the synthesized complexes. Gram magnetic susceptibility and molar magnetic moment values were calculated and used to compute the effective magnetic moments of all the complexes. Generally, square

planer Ni(II) complexes are diamagnetic, while octahedral and tetrahedral complexes are paramagnetic with magnetic moment of 2.8 – 3.4 and 3.4 – 4.0 B.M respectively. In this study Ni(II) complex has a magnetic moment of 2.91 B.M which indicate two unpaired electrons in octahedral environment [33]. A magnetic moment of 1.7 – 2.2 B.M is usually observed for mononuclear Cu(II) complexes regardless of their geometries. i.e. (t_2g^6, eg^3) sometimes the values are higher than the spin only moment, likely due to orbitals contribution and spin orbit coupling [31]. In this study the Cu(II) complex has a total effective magnetic moment of 1.76 B.M indicative of one unpaired electron observable for six coordinate octahedral geometry [29]. Zn(II) complex is diamagnetic with negative molar susceptibility value. The complex assumed six coordinate geometry [30].

Table 4 show the infrared spectral data of the dihydrazone B and its complexes. The υ(O-H) absorption band for water of crystallization were observed at 3327 cm^{-1}, 3365 cm^{-1} and 3342 cm^{-1} in the spectra of Ni(II), Cu(II) and Zn(II) complexes respectively. The υ(N-H) absorption band in the spectrum of dihydrazone was observed at 3309 cm^{-1}, which were observed in the range of 3238 – 3253 cm^{-1} in the spectra of the complexes [31]. So also, υ(C=O) stretching frequency for the dihydrazone was seen at 1674 cm^{-1} and for the complexes between 1659 – 1666 cm^{-1}. The strong absorption band at 1603 cm^{-1} in the spectrum of the dihydrazone is due to υ(C=N) which was shifted to 1626 – 1629 cm^{-1} in the spectra of the complexes due to coordination through nitrogen atom of azomethine group [31]. New absorption bands at 515 - 540 cm^{-1} and 415 - 474 cm^{-1} in the spectra of the complexes were due to υ(M-N) and υ(M-Cl) respectively. This confirm the coordination of the dihydrazone to the metal ions. The result is similar with the results reported by Karthika *et al.,* [1] and Racheal *et al.,* [3]. UV-visible spectra of the dihydrazone and that of its complexes were recorded and presented in Table 5. The dihydrazone B spectrum displayed high-pitched absorption bands, λmax (nm) attributed to the following electronic transitions.,. 206 (π - π* aromatic ring), 249 (π - π* C=O), 268 (π - π* C=N), 336 (n - π* C=O) and 383 nm (n - π* C=N). These are consistent with the results stated by Ayman *et al.,* [24]. The complexes showed high intensities electronic transitions at 207 - 220 (π - π* aromatic ring), 253 - 260 (π - π* C=O), 279 - 285 (π - π* C=N), 343 - 369 (n - π* C=O) and 367 – 379 nm (n - π* C=N). The shift in absorption bands to lower λ_{max} (blue shift) or higher λ_{max} (red shift) in the spectra of the complexes are due to coordination of the dihydrazone to the metal ions. These are comparable to the results reported by Idris *et al.,* [33].

The results for elemental analysis of the dihydrazone and that of the metal(II) complexes were presented in Table 6. The experimental values obtained were in good agreement with the calculated percentages of C, H and N in the compounds. The variation was insignificant. This agrees with the proposed structures of the complexes, that is, 1:2 metal to ligand ratio. These were in good agreement with the results reported by Uba [32]. The dihydrazone B has a molecular formula of $C_{18}H_{14}N_4O_6$ with molecular weight of 382 g/mol. The mass spectrum of the compound displayed the molecular ion peak at m/z 383 in a positive mode due to $[M + H]^+$ ion, this is explicitly in good agreement with the molecular mass of the compound. The mass spectrum of the ligand also exhibits peaks assigned to its different fragments. Some of the identified fragments include $C_{10}H_8N_2O_4$, $C_9H_8N_2O_3$, $C_9H_9N_3O_2$, $C_8H_8N_2O_2$, $C_9H_{10}N_2O$ and $C_8H_8O_2$ that were observed at m/z 220, 192, 191, 164, 162 and 136 respectively [28]. This are in accordance with the structure of the synthesized compound, and the mass spectrum is shown in figure 1.

The TGA curve of dihydrazone B $C_{18}H_{14}N_4O_6$ revealed two sequential stages of weight loss. The first stage befell within the temperature range of 250 - 270 °C, resulting in a weight loss of 11.39% (calculated 11.51%) which corresponds to the loss of CO_2 molecule, the DTG curve gave maximum temperature peak at 260 °C. This observation confirmed the existence of oxygen atoms in the oxalyldihydrazone B ligand. Stage 2 was detected between 320 - 350 °C which led to a weight loss of 88.26 % (calculated 88.48 %), attributed to the loss of $C_{17}H_{14}N_4O_4$ molecule where the DTG curve gave a maximum peak temperature at 350 °C comparable to the results reported by Ayman *et al.,* [24] and Hassan *et al.,* [23].

Fig. 3 and 4 show the *in-vitro* antibacterial and antifungal activities of the dihydrazone and its metal(II) complexes. The compounds were tested against three clinically isolated pathogenic bacteria (*Staphylococcus aureus, Escherichia coli* and *Salmonella typhi*), and three fungal strains (*Aspergillus fumigitus, Aspergillus niger* and *Aspergillus flavus*). The results indicated that, the metal complexes exhibit higher antibacterial and antifungal activities than the free dihydrazone. The presence of metal ions increases the activity of the compound. Incorporation of metal ions into the ligands increases its liposolubility (lipid soluble). According to Overtone's concept of cell permeability, the lipid membrane that surrounds the microbial cells favours the passage of only lipid soluble materials, due to which, liposolubility is an important factor, that determine the antibacterial and antifungal activities of the tested compounds [3]. The variation in the effectiveness of different compounds against different organisms depends either on the permeability of the microbial cells or on

differences in ribosome of microbial cells. That is the reason why some compounds are more potent against microbes than others [1]. Moreover, the activity is concentration dependent, it increases generally, with increase in concentrations. But their activities are comparable with that of control, as indicated in Figures 5 and 6.

All the compounds are more potent against gram-positive *staphylococcus aureus* than gram-negative *Escherichia coli* and *Salmonella typhi. T*his is because, lipid and lipoprotein content is low in the cell wall of gram positive bacteria which facilitate the penetration of the compound through the cell of the microbes which may eventually result in the death of the cells. Hence, the cell wall of the gram positive bacteria is more prone to disruption by the tested compounds [34]. However, lipid and lipoprotein content is high in the cell wall of gram negative bacteria, which make the penetration of the compound into the bacterial cells so difficult and sometimes impossible. This phenomenon is the cause of drugs resistance by many gram negative bacteria. Additionally, the compounds have higher inhibition capacity against *Aspergillus fumigitus,* and moderate activity against *Aspergillus niger* but have lesser or mild activity on *Aspergillus flavus.* These were in agreement with the results reported by Suleiman *et al.,* [29].

The dihydrazone B ligand and the complexes were screened for their antioxidant potential using DPPH assay, in which the result is presented in Figure 5. The antioxidant activity results exhibit that the % radical scavenging power increases with increase in concentration of the tested compounds. The percentage radical scavenging potential of the ligand (dihydrazone B) was 70.85 % at 1000 µg/mL which got enhanced on complexation with metal ions to 83.94% in the case of copper complex [7]. Among the screened compounds, the ligand possesses very low radical scavenging activity with (IC50 = 60.29 ± 0.02 µg/mL) as compared to the standard ascorbic acid (IC50 = 2.82 ± 0.01 µg/mL). The results were shown in Figure 6. The complexes generally showed enhanced scavenging activity. (IC50 = 39.02 ± 0.06, 12.89 ± 0.03 and 44.56 ± 0.07 µg/mL) for Ni(II), Cu(II) and Zn(II) complexes respectively. Copper(II) complex exhibited higher scavenging activity than the other complexes, but comparable to the standard antioxidant (ascorbic acid), similar to the results reported by Nighat *et al.,* [28].

The synthesized compounds were subjected to *in-vitro a*nti-inflammatory activity using albumin inhibition denaturation technique according to Karthik *et al.,* [1] with slight modification. All the complexes exhibited significant anti-inflammatory action. Cu(II) and Zn(II) complexes have comparable anti-inflammatory activity with the standard diclofenac

sodium as shown in Figure 7. The Zn(II) complex has the highest percent inhibition of 90 % at 2000 µg/mL and is found to be most significant with IC50 231.99 µg/mL. From the overall percentage inhibition, all the complexes have displayed enhanced and significant anti-inflammatory activity, that are comparable or equipotent with the standard drug, diclofenac sodium.

CONCLUSION

The dihydrazone and its respective biologically active complexes were successfully synthesized and characterized by different physicochemical techniques and spectral analysis. All the synthesized compounds were obtained in appreciable yield with significant thermal stability. The complexes are non-electrolytic due to low values of molar conductance. The values of effective magnetic moment indicate the paramagnetic nature of the complexes with the exception of zinc(II) complex. Infrared spectra show all the prominent absorption bands at the desired wave number. Electronic spectra show π - π^* and n - π^* transitions at expected wavelength values. Additionally, the results for elemental analyses show 1:2 metal to ligand ratio which are in good agreement with the proposed structures. The dihydrazone and all the complexes display appreciable activities against pathogenic bacterial and fungal species, as such the compounds are potent antimicrobial agents. Furthermore, they exhibit remarkable radical scavenging and significant anti-inflammatory activities, indicating their potency as good antioxidant and effective anti-inflammatory agents.

REFERENCES

[1] Karthik, S., Priyab, P. & Gomathi, T. (2024). Synthesis, characterization, antimicrobial, anti-diabetic, anti-inflammatory and anti-cancer studies of Schiff base metal(II) complexes derived from mixed Schiff base ligands *Indian Journal of Chemistry* 63. 112-120. Doi: 10.56042/ijc.v63i1.4556.

[2] Feldman, C. & Anderson, R. (2021). The role of co-infections and secondary infections in patients with Covid-19. *Pneumonia*, 13 (5), 1-5 Doi:10.1186/s41479-021-00083-w

[3] Racheal, O. A., Ikechukwu, P. E. & Hadley, S. C. (2023). Schiff base metal complexes as a dual antioxidant and antimicrobial agents. *Journal of Applied Pharmaceutical Science* 13 (03), 132 - 140. DOI: 10.7324/JAPS.2023.91056

[4] Ejidike, I. P., Mtunzi, M. & Klink, M. J (2019). Spectroscopic, XRD, *in vitro* Antioxidant Antifungal and Antibacterial Studies of Heterocyclic Schiff base Nickel(II) Complexes Bearing Anions. *Springer, Cham, Switzerland*. 283 - 305.

[5] Bamigboye, O. M., Ejidike, I. P., Lawal, M., Nnabuike, G. G. & Clayton, H. S. (2021). Mixed amodiaquine-acetylsalicylic acid metal complexes: characterization and anti-microbial potentials. *Sci Technol Asia*. 26(1), 53 - 63.

[6] Jain, P., Pandey, G., Kumar, D. & Chandra, S. (2019). Prospects of biologically active Schiffbase ligand and metal complexes in drug discovery, *Adv. Sci. Eng. Med.* 11 (1), 144 - 154

[7] Adole, V.A., More, R.A., Jagdale, B.S., Pawar, T.B. & Chobe, S.S. (2020). Efficient synthesis, antibacterial, antifungal, antioxidant and cytotoxicity study of 2-(2-hydrazineyl) thiazole derivatives. *Chem Select.* 5(9). 2778 - 2786

[8] Ejidike, I.P., Bamigboye, O.M. & Clayton, H.S. (2021). Spectral, in vitro antiradical and antimicrobial assessment of copper complexes containing tridentate Schiff base derived from dihydroxybenzene functionality with diaminoethylene bridge. *Spectrosc Lett,*54 (3), 212 - 230.

[9] Hashem, H.E. Nath, A. & Kumer, A. (2022). Synthesis, molecular docking, molecular dynamic quantum calculation, and antibacterial activity of new Schiff base metal complexes, *J. Mol. Struct.* 1250 Pp. 1-13. Doi.org/10.1016/j.molstruc.2021.131915

[10] Shi, J. (2022). Synthesis, characterization, crystal structure and antibacterial activity studies of cobalt (II) and zinc (II) complexes containing halogen quinoline Schiff base ligand, *J. Mol. Struct.* 1253. Doi.10.1016/j.molstruc.2021.132263

[11] Noma, S. A. A. (2020). Synthesis, characterization and biological assessment of a novel hydrazone as potential anticancer agent and enzyme inhibitor, *J. Mol. Structure.* 12 (11).

[12] Nfor, E. N., Husian, A., Majoumo, F., Njah, I. N., Offiong, O. E. & Bourne, S. A. (2023). Synthesis, crystal structure and antifungal activity of a Ni (II) complex of a new hydrazone derived from antihypertensive drug hydralazine hydrochloride, *Polyhedron* 63, 207 - 213.

[13] Cukurovali, A (2023). Synthesis, antibacterial and antifungal activity of some new thiazolylhydrazone derivatives containing 3-substituted cyclobutane ring, *Eur. J. Med. Chem.* 41 (2). 201 - 207.

[14] Bitu, M.N.A. (2019). Anti-pathogenic activity of Cu (II) complexes incorporating Schiff bases: a short review, *Am. J. Heterocycl. Chem.* 5 (1), 11 - 23.

[15] Liu, W. Y., Li, H.Y., Zhao, B. X., Shin, D. S.., Lian, S. & Miao, J.Y. (2023). Synthesis of novel ribavirin hydrazone derivatives and anti-proliferative activity against A549 lung cancer cells, *Carbohydr. Res.* 344 (11), 1270 - 1275.

[16] Mohamed, G. G., Omar, M. M. A., Moustafa, B. S., AbdEl-Halim, H. F. & Farag, N. A. (2022). Spectroscopic investigation, thermal, molecular structure, antimicrobial and anticancer activity with modelling studies of some metal complexes derived from isatin Schiff base ligand, *Inorg. Chem. Commun.* 141 109606.

[17] Musad, E.A., Mohamed, R., Ali S. B., Vishwanath, B.S. & Lokanatha, R. K. (2023). Synthesis and evaluation of antioxidant and antibacterial activities of new substituted bis (1, 3, 4-oxadiazoles), 3, 5-bis (substituted) pyrazoles and isoxazoles, *Bioorg. Med. Chem. Lett.* 21 (12), 3536 - 3540.

[18] Ali, A., Khalid, M., Abid, S., Tahir, M., Iqbal J., Ashfaq, M., Lu, C. & Rehman, M (2020). Green synthesis, SC-XRD, non-covalent interactive potential and electronic communication via DFT exploration of pyridine-based hydrazone, *Crystals* 10 (9),778.

[19] Angelova, V (2016). Recent developments of hydrazide/hydrazone derivatives and their analog as anticonvulsant agents in animal models, *Drug Dev. Res.* 77 (7). 379-392.

[20] Le, T. & Thuy, (2022). Design, synthesis and *in vitro* antimalarial evaluation of new quinolinylhydrazone derivatives, *Lett. Drug Des. Discovery* 9 (2), 163 - 168.

[21] Gowdhami, B., Manojkumar, Y., Vimala, R.V., Ramya, V., Karthiyayini, B., Kamal, B. & Akbarsha, M.A (2022). Cytotoxic Cobalt (III) Schiff Base Complexes: *In-vitro* Anti-proliferative, Oxidative Stress and Gene Expression Studies in Human Breast and Lung Cancer Cells. *Biometals*. 35, 67-85.

[22] Shaikh, I., Travadi, M., Jadeja, R.N., Butcher, R.J. & Pandya, J.H. (2022). Crystal feature and spectral characterization of Zn (II) complexes containing Schiff base of Acylpyrazolone ligand with antimalarial action, *J. Indian Chem. Soc.* 99 (5). Doi: 10.3390/ijms232314840.

[23] Hassan, A.M., Ayman, H. A., Hosni, A. G., Bassem, H. M. & Ahmed, M. E. (2018). Mn^{2+} Complexes of N,O-Dihydrazone: Structural Studies, Indirect Band Gap Energy and Corrosion Inhibition on Aluminum in Acidic Medium. *J. Chil. Chem. Soc.*, 63 (4): 4180 – 4189.

[24] Ayman, H. A., Hassan A. M., Hosni A. G., Bassem H. M., Ahmed M. E. & Ahmed A. O. (2019). Copper(II)-oxaloyldihydrazone complexes: Physico-chemical studies: Energy band gap and inhibition evaluation of free oxaloyldihydrazones toward the corrosion of copper metal in acidic medium**.** *Arabian Journal of Chemistry* 12. Pp. 4287 – 4302.

[25] Mouayed, Y.K and Abduljleel, M. A (2024). Synthesis, characterization and biological studies of schiff bases derived from piperonaldehyde and their complexes with cobalt (II) *Der Pharma Chemica,* 6(5): Pp. 88 - 100.

[26] Laxman, V. G., Ali, A. M., Muataz, J.K.A., Shashikant, H. G., Makarand, K., Rajesh D & Panchsheela, A. U (2024). Novel terephthalaldehyde bis(thiosemicarbazone) Schiff base ligand and its transition metal complexes as antibacterial Agents: Synthesis, characterization and biological investigations. *Results in Chemistry 101316.* doi.org/10.1016/j.rechem.2024.101316

[27] Bhagwat, V., Digambar, K. & Avinash, S (2022). Synthesis, spectral studies, antioxidant and antibacterial evaluation of aromatic nitro and halogenated tetradentate Schiff bases. *Heliyon 8*. Doi.org/10.1016/j.heliyon.2022.e09650

[28] Nighat, N., Irshad, A., Nizam, M. D., Amjad, W. & Sadeeq, U. (2020). Synthesis, Characterization and Antioxidant Activity of Nickel(II) Schiff Base Complexes Derived from 4-N,N-(Dimethylamino)benzaldehyde. *Journal of the Chemical Society of Pakistan*. 42 (2), 238- 242. https://hal.science/hal-02563496

[29] Suleiman, A. K., Sadi, A. H., Hadiza, A. & Aminu, D. (2023). Synthesis, Characterization and Antimicrobial Evaluation of Schiff Base Transition Metal Complexes of (E)-2-((2- methoxybenzylidene)amino)Phenol *Nigerian Research Journal of Chemical Sciences* (ISSN: 2682-6054) 11 (2): 100 – 114.

[30] Khaleel, S A., Sadi A. H., Badamasi, H. & Ahmadu, M. (2023). Synthesis, Characterization and Antimicrobial Studies of Schiff Base Derived from 2-Amino Phenol and O-Anisaldehyde and Its Co (II), Cu (II) and Zn (II) Complexes. *Dutse Journal of Pure and Applied Sciences (DUJOPAS)*, 9 (2a), 301 – 310.

[31] Sayeed, A., Na'aliya, J. & Ethan, W. (2022) Synthesis, Characterization and Antimicrobial Studies of Metal(II) complexes with 4-methoxybenzaldehyde with p-anisidine, *Global Journal of Pure and Applied Chemistry Research*, 10 (1), 23-38.

[32] Uba, B (2022). Synthesis, Characterization and Antimicrobial Activities of Schiff Base Complexes of Co (II) and Cu (II) Derived from Salicyldehyde and Diphenylamine. Scholars International Journal of Chemistry and Material Sciences. 5(1): 6 – 10. DOI: 10.36348/sijcms.2022.v05i01.002

[33] Idris, M. I., Sadi A. H. & Abubakar, A. A. (2020). Synthesis, Characterization and Biological Studies of Ni(II) Complexes with Schiff Base Co-ligand Derived from 5,6-Diaminophenanthroline and Benzene-1,4-Dicarbaldehyde. *FUDMA Journal of Sciences (FJS).* 4 (3), 132 -141.

[34] Lakna, P. (2017). Difference Between Gram Positive and Gram Negative Bacteria. *EPEDIAA.* Retrieved via http://pediaa.com/difference-between-gram-positive-and-gram-negative-bacteria on 4th August, 2024.